

Atmospheric chemistry of benzaldehyde: UV absorption spectrum and reaction kinetics and mechanisms of the C₆H₅C(O)O₂ radical

Françoise Caralp,^a Virginie Foucher,^a Robert Lesclaux,^{*a} Timothy J. Wallington^{*b} and Michael D. Hurley^b

^a Laboratoire de Physico-Chimie Moléculaire, Université Bordeaux I, UMR 5803 CNRS, 33405 Talence, France. E-mail: lesclaux@cribx.u-bordeaux.fr

^b Ford Research Laboratories MD 3083/SRL, Ford Motor Company, Dearborn, Michigan 48121-2053, USA. E-mail: twallington@ford.com

Received 19th April 1999, Accepted 10th June 1999

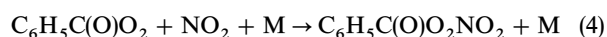
Flash photolysis–UV absorption and long pathlength FTIR–smog chamber studies of several reactions involving C₆H₅C(O) and C₆H₅C(O)O₂ radicals have been performed. It was determined that reaction of Cl atoms with C₆H₅CHO proceeds *via* abstraction of the aldehydic hydrogen to give benzoyl radicals. The sole atmospheric fate of benzoyl radicals is addition of O₂ to give peroxybenzoyl radicals. Reaction of C₆H₅C(O) radicals with molecular chlorine proceeds with a rate constant of $(5.9 \pm 0.4) \times 10^{-11} \text{ cm}^3 \text{ molecule}^{-1} \text{ s}^{-1}$ at 296 K and 1–700 Torr total pressure. The UV spectrum of C₆H₅C(O)O₂ radicals (245–300 nm) and the self reaction were investigated simultaneously, yielding $\sigma_{\text{max}} = (2.0 \pm 0.1) \times 10^{-17} \text{ cm}^2 \text{ molecule}^{-1}$ at 245 nm and $k_{16} = (3.1 \pm 1.4) \times 10^{-13} \exp[(1110 \pm 160) \text{ K}/T] \text{ cm}^3 \text{ molecule}^{-1} \text{ s}^{-1}$, measured from 298 to 460 K. At 338 K, C₆H₅C(O)O₂ radicals react with NO with a rate constant of $(1.6 \pm 0.4) \times 10^{-11} \text{ cm}^3 \text{ molecule}^{-1} \text{ s}^{-1}$. At 296 K, C₆H₅C(O)O₂ radicals react with NO₂ with a rate constant of $(1.1 \pm 0.3) \times 10^{-11} \text{ cm}^3 \text{ molecule}^{-1} \text{ s}^{-1}$ to form C₆H₅C(O)O₂NO₂, which undergoes thermal decomposition at a rate of $k_{-4} = (2.1^{+5.0}_{-1.5}) \times 10^{16} \exp[-(13\,600 \pm 400) \text{ K}/T] \text{ s}^{-1}$ in one atmosphere of air. At 296 K in 100–700 Torr of air $k[\text{C}_6\text{H}_5\text{C(O)O}_2 + \text{NO}]/k[\text{C}_6\text{H}_5\text{C(O)}_2 + \text{NO}_2] = 1.44 \pm 0.15$. Relative rate methods were used to measure $k[\text{Cl} + \text{C}_6\text{H}_5\text{C(O)Cl}] = (1.1 \pm 0.2) \times 10^{-15} \text{ cm}^3 \text{ molecule}^{-1} \text{ s}^{-1}$ at 296 K. Uncertainty limits are all two standard deviations. Results are discussed with respect to the literature data and the atmospheric chemistry of benzaldehyde.

1 Introduction

Aromatic compounds are an important class of organic compounds found in gasoline and vehicle exhaust which contribute to the formation of ozone¹ and secondary organic aerosol² in urban air. Benzaldehyde is an intermediate in the atmospheric oxidation of aromatic compounds and has been identified in polluted air in many locations around the world. Benzaldehyde is removed from the atmosphere by reaction with OH, to produce the peroxybenzoyl radical, C₆H₅C(O)O₂:



As with other peroxy radicals, C₆H₅C(O)O₂ reacts with nitrogen oxides in polluted atmospheres. Reaction with NO gives the benzoyloxy radical, while reaction with NO₂ gives peroxybenzoyl nitrate, C₆H₅C(O)O₂NO₂, a lacrymator³ that has been detected in photochemical smog:⁴



Kenley and Hendry⁵ have measured $k_3/k_4 = 1.52 \pm 0.12$ in 800 Torr of Ar at 303.6 K, while Kirchner *et al.*⁶ report $k_3/k_4 = 1.59 \pm 0.20$ in 740 Torr of N₂ at 310–322 K. There are no absolute kinetic data available for either k_3 or k_4 , or indeed for any reaction of the C₆H₅C(O)O₂ radical.

To improve our understanding of the atmospheric chemistry of benzaldehyde in particular, and aromatic compounds in general, we have conducted kinetic and mechanistic studies of a variety of atmospherically significant reactions involving C₆H₅C(O) and C₆H₅C(O)O₂ radicals. The UV absorption spectrum of C₆H₅C(O)O₂ radicals over the wavelength range 245–300 nm was recorded in Bordeaux. Absolute rate kinetic studies were conducted in Bordeaux over the temperature range 298–460 K for the C₆H₅C(O)O₂ radical self reaction and its reaction with NO. Relative rate and product studies were performed at Ford of the reactions of C₆H₅C(O) radicals with O₂ and Cl₂, and C₆H₅C(O)O₂ radicals with NO and NO₂.

2 Experimental

2.1 FTIR experiments at Ford Motor Company

Experiments were performed in a 140 litre Pyrex reactor interfaced to a Mattson Sirius 100 FTIR spectrometer.⁷ The reactor was surrounded by 22 fluorescent blacklamps (GE F15T8-BL), which were used to photochemically initiate the experiments. Peroxybenzoyl radicals were generated by the photolysis of molecular chlorine in the presence of benzaldehyde in O₂/N₂ mixtures at 700 Torr total pressure at $296 \pm 2 \text{ K}$.

The loss of benzaldehyde and the formation of products were monitored by Fourier transform infrared (FTIR) spectroscopy using an infrared pathlength of 27 m, and a resolution of 0.25 cm⁻¹. Infrared spectra were derived from 32

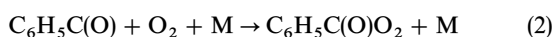
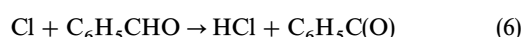
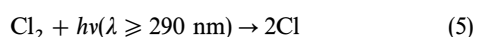
co-added interferograms. Reference spectra were obtained by expanding known volumes of the reference material into the long pathlength cell. Products were identified and quantified by fitting reference spectra of the pure compounds to the observed product spectra using integrated absorption features over the following wavelength ranges (in cm^{-1}): benzaldehyde, 775–850 and 1700–1750; benzoyl chloride, 740–1850; peroxybenzoyl nitrate, 900–1400; and CO_2 , 2300–2400.

Six sets of experiments were performed. First, a relative rate technique was used to determine the rate constant for the reaction of Cl atoms with $\text{C}_6\text{H}_5\text{C(O)Cl}$. Second, the mechanism of the reaction of Cl atoms with benzaldehyde was investigated by irradiating $\text{C}_6\text{H}_5\text{CHO}/\text{Cl}_2/\text{N}_2$ mixtures and quantifying the formation of $\text{C}_6\text{H}_5\text{C(O)Cl}$. Third, the relative reactivity of benzoyl radicals towards Cl_2 and O_2 was studied by irradiating $\text{C}_6\text{H}_5\text{CHO}/\text{Cl}_2/\text{N}_2/\text{O}_2$ mixtures and observing the dependence of the yield of $\text{C}_6\text{H}_5\text{C(O)Cl}$ on the concentration ratio $[\text{O}_2]/[\text{Cl}_2]$. Fourth, the relative reactivity of peroxybenzoyl radicals towards NO and NO_2 was investigated by irradiating $\text{C}_6\text{H}_5\text{CHO}/\text{Cl}_2/\text{NO}/\text{NO}_2$ mixtures and observing the dependence of the yield of $\text{C}_6\text{H}_5\text{C(O)O}_2\text{NO}_2$ on the $[\text{NO}]/[\text{NO}_2]$ concentration ratio. Fifth, the rate of thermal decomposition of $\text{C}_6\text{H}_5\text{C(O)O}_2\text{NO}_2$ was measured. Finally, the products following the Cl atom initiated oxidation of benzaldehyde in air in the presence of NO_x were investigated.

Initial concentrations of the gas mixtures for the relative rate experiments were 5–25 mTorr of the reactant and reference organics with 100 mTorr of Cl_2 in 700 Torr of N_2 diluent. In the product study mixtures of 6–9 mTorr of benzaldehyde, 200–300 mTorr of Cl_2 , 16.6–45.9 mTorr of NO, in 700 Torr of air diluent, were used. All reagents were purchased from commercial vendors at purities of >99% and were used without further purification.

2.2 Flash photolysis experiments at Université Bordeaux I

The flash photolysis–UV absorption technique used in this work is described in detail elsewhere.⁸ Peroxybenzoyl radicals were generated from the flashlamp photolysis of Cl_2 at wavelengths above the Pyrex cut-off, in the presence of benzaldehyde:



As shown in Section 3.2, the reaction of Cl atoms with benzaldehyde proceeds *via* H-atom abstraction from the –CHO group.

The gas mixture, composed of $\text{C}_6\text{H}_5\text{CHO}/\text{Cl}_2/\text{O}_2/\text{N}_2$ mixtures, was slowly flowing through a cylindrical quartz cell (70 cm long), and the cell mixture was replenished between successive flashes. All experiments were performed at atmospheric pressure. The temperature of the cell was controlled to ± 3 K using a surrounding electrically heated oven. The photolysis radiation was produced over a time scale of a few microseconds by discharging an argon flashlamp situated outside and running parallel to the cell. Short wavelengths ($\lambda < 290$ nm) were eliminated using a Pyrex filter. The analysis beam from a deuterium lamp passed through the cell and impinged onto a monochromator/photomultiplier unit. Individual experimental absorption curves were fed into a transient recorder and passed to a microcomputer for averaging and further analysis. The number of co-added absorption curves required to obtain a good signal-to-noise ratio was between 15 and 50.

The concentration of molecular chlorine was determined from its UV absorption at 330 nm ($\sigma = 2.56 \times 10^{-19} \text{ cm}^2 \text{ molecule}^{-1}$)⁹ and was varied over the range $(0.7\text{--}3.0) \times 10^{16}$

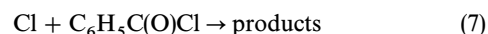
molecule cm^{-3} . The resulting initial radical concentrations were in the range $(0.8\text{--}6.0) \times 10^{13} \text{ molecule cm}^{-3}$. Benzaldehyde was introduced into the gas phase by bubbling a small fraction of the carrier gas flow through liquid benzaldehyde maintained at 288 K. The $\text{C}_6\text{H}_5\text{CHO}$ concentration was estimated from the diluent flow rate and $\text{C}_6\text{H}_5\text{CHO}$ vapour pressure (0.44 Torr at 288 K). Benzaldehyde concentrations of $(0.4\text{--}1.5) \times 10^{15} \text{ cm}^{-3}$ were used. These concentrations were sufficient to ensure that reaction with benzaldehyde was the dominant fate of Cl atoms ($k_6 = 9.6 \times 10^{-11} \text{ cm}^3 \text{ molecule}^{-1} \text{ s}^{-1}$)¹⁰ while low enough that absorption by benzaldehyde in the wavelength range of interest was not a major problem. Conversion of Cl atoms into peroxybenzoyl radicals was complete within a few microseconds, *i.e.* on a time scale much shorter than the subsequent radicals reactions. During the course of experiments conducted at room temperature, the analysing light intensity decreased after a few hours, probably as a result of product deposition on the inner surfaces of the cell. This could be avoided by heating the cell to approximately 340 K, and thus most experiments were performed around this temperature rather than at room temperature. Kinetic simulations were performed by numerical integration and fitted to the decay traces using nonlinear least-squares analysis.

Synthetic air (AGA Gaz speciaux), chlorine (5% in N_2 , AGA Gaz speciaux), benzaldehyde (Aldrich 99%), NO (AGA Gaz Speciaux, 0.96% in N_2 , purity >99.9%) oxygen (>99.5%) and nitrogen (AGA, >99.995%) were all used without further purification. Gas flow rates were measured and regulated by calibrated Tylan flow controllers.

3 Results

3.1 Rate constant for Cl + $\text{C}_6\text{H}_5\text{C(O)Cl}$

As a preliminary exercise prior to investigating the mechanism of reaction of Cl atoms with $\text{C}_6\text{H}_5\text{CHO}$, the rate constant for reaction of Cl atoms with $\text{C}_6\text{H}_5\text{C(O)Cl}$ was measured relative to the reactivity of Cl atoms with CD_4 and HFC-236cb ($\text{CF}_3\text{CF}_2\text{CFH}_2$) using the FTIR technique described previously.¹¹ Experiments were performed in which $\text{C}_6\text{H}_5\text{C(O)Cl}/\text{CD}_4/\text{N}_2/\text{Cl}_2$ and $\text{C}_6\text{H}_5\text{C(O)Cl}/\text{HFC-236cb}/\text{N}_2/\text{Cl}_2$ mixtures were subjected to UV irradiation with the decay of $\text{C}_6\text{H}_5\text{C(O)Cl}$ and the reference compounds monitored using FTIR spectroscopy. Control experiments were performed to check for loss of $\text{C}_6\text{H}_5\text{C(O)Cl}$ *via* photolysis in the chamber and heterogeneous loss. Mixtures of $\text{C}_6\text{H}_5\text{C(O)Cl}$ in N_2 were prepared, left to stand for 5 min in the dark, and then subject to UV irradiation for 5 min; there was no discernible (<2%) loss of $\text{C}_6\text{H}_5\text{C(O)Cl}$. Similar control experiments have shown that photolysis and heterogeneous loss of CD_4 and HFC-236cb are also of no significance. Fig. 1 shows the observed decay of $\text{C}_6\text{H}_5\text{C(O)Cl}$ *vs.* those of CD_4 and HFC-236cb when mixtures of these compounds were exposed to Cl atoms in 700 Torr of N_2 diluent at 296 K. Linear least-squares analysis gives ratios of $k_7/k_8 = 0.19 \pm 0.02$ and $k_7/k_9 = 0.73 \pm 0.10$:



Taking $k_8 = 6.1 \times 10^{-15}$ (ref. 11) and $k_9 = 1.5 \times 10^{-15} \text{ cm}^3 \text{ molecule}^{-1} \text{ s}^{-1}$ (ref. 12) gives $k_7 = (1.16 \pm 0.12) \times 10^{-15}$ and $(1.10 \pm 0.15) \times 10^{-15} \text{ cm}^3 \text{ molecule}^{-1} \text{ s}^{-1}$. We choose to quote a final value of k_7 that is the average of the two determinations together with uncertainties which encompass the extremes of the uncertainty ranges of the individual determinations, hence $k_7 = (1.1 \pm 0.2) \times 10^{-15} \text{ cm}^3 \text{ molecule}^{-1} \text{ s}^{-1}$.

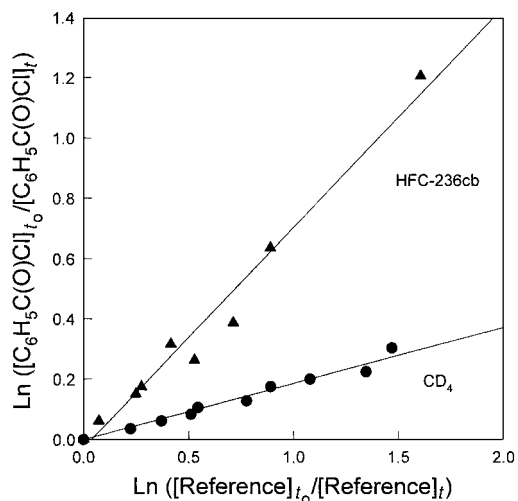


Fig. 1 Decay of benzoyl chloride *vs.* HFC-236cb (triangles) and CD_4 (circles) in the presence of Cl atoms in 700 Torr of air at 296 K.

We estimate that potential systematic errors associated with uncertainties in the reference rate constants could add an additional 10% uncertainty. There are no literature data to compare with this result.

3.2 Mechanism of the Cl + $\text{C}_6\text{H}_5\text{CHO}$ reaction

To investigate the mechanism of reaction of Cl atoms with benzaldehyde, mixtures of 6–12 mTorr of benzaldehyde and 20–100 mTorr of chlorine were subject to successive short (0.5–1 s) irradiations in 700 Torr of N_2 diluent at 296 K in the FTIR system. In these experiments it was observed that benzaldehyde was converted into benzoyl chloride. After subtraction of features ascribed to benzoyl chloride no residual IR features remained. Fig. 2 shows a plot of the observed formation of benzoyl chloride *vs.* the loss of benzaldehyde. Linear least-squares analysis gives a benzoyl chloride yield of $100 \pm 5\%$. This result is consistent with the photochemical chain chlorination of benzaldehyde *via* reactions (6) and (10):



The 100% yield of $\text{C}_6\text{H}_5\text{C}(\text{O})\text{Cl}$ and the absence of any IR features other than those attributable to $\text{C}_6\text{H}_5\text{C}(\text{O})\text{Cl}$ in the

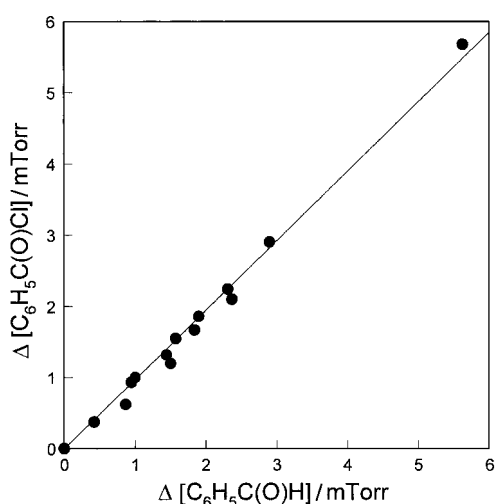


Fig. 2 Observed formation of benzoyl chloride *vs.* loss of benzaldehyde following the UV irradiation of benzaldehyde/ Cl_2/N_2 mixtures.

product spectra show that the reaction of Cl atoms with benzaldehyde proceeds *via* abstraction of the aldehydic H atom. A control experiment was performed to check for photolysis of benzaldehyde in the FTIR–smog chamber system. An 11 min irradiation resulted in a 12% loss from which we calculate a photolysis rate of $2 \times 10^{-4} \text{ s}^{-1}$. The irradiation times used in all experiments were sufficiently short (0.5–30 s) that photolysis of benzaldehyde is of negligible importance.

3.3 Relative reactivity of $\text{C}_6\text{H}_5\text{C}(\text{O})$ radicals towards Cl_2 and O_2

The rate constant ratio k_{10}/k_2 was measured using the FTIR–smog chamber system by irradiating $\text{C}_6\text{H}_5\text{CHO}/\text{Cl}_2/\text{O}_2/\text{N}_2$ mixtures and observing the dependence of the yield of benzoyl chloride on the $[\text{Cl}_2]/[\text{O}_2]$ concentration ratio:



As the $[\text{O}_2]/[\text{Cl}_2]$ concentration ratio was increased the yield of benzoyl chloride was suppressed. This behavior is expected as the additional O_2 competes with reaction (10) for the available $\text{C}_6\text{H}_5\text{CO}$ radicals. Experiments were performed at total pressures of 1–700 Torr (N_2 diluent) with the concentration ratio $[\text{Cl}_2]/[\text{O}_2]$ varied over the range 0.02–0.16. As discussed elsewhere,¹³ a plot of $Y_{\text{C}_6\text{H}_5\text{C}(\text{O})\text{Cl}}/(1 - Y_{\text{C}_6\text{H}_5\text{C}(\text{O})\text{Cl}})$ *vs.* $[\text{Cl}_2]/[\text{O}_2]$, where $Y_{\text{C}_6\text{H}_5\text{C}(\text{O})\text{Cl}}$ is the molar yield of benzoyl chloride, $\Delta[\text{C}_6\text{H}_5\text{C}(\text{O})\text{Cl}]/\Delta[\text{C}_6\text{H}_5\text{CHO}]$, should be linear, pass through the origin, and have a slope of k_{10}/k_2 . Fig. 3 shows such a plot. There was no discernible effect of total pressure over the range 1–700 Torr suggesting reaction (2) is at, or near, the high pressure limit over this pressure range. Such behavior is reasonable considering the kinetic data base for alkyl radicals of this size.¹⁴ Linear least-squares analysis of the data in Fig. 3 gives $k_{10}/k_2 = 10.4 \pm 0.6$. Combination of this result with the measurement¹⁵ of $k_2 = 5.7 \times 10^{-12}$ gives $k_{10} = (5.9 \pm 0.4) \times 10^{-11} \text{ cm}^3 \text{ molecule}^{-1} \text{ s}^{-1}$. We estimate that potential systematic errors associated with uncertainties in k_2 could add an additional 20% uncertainty to the determination of k_{10} . The present study is focused on the chemistry of peroxybenzoyl radicals. In the subsequent experiments it was important to choose experimental conditions where chloride formation is minimal. The fraction of benzoyl radicals that react with O_2 is given by $1/(1 + 10.4[\text{Cl}_2]/[\text{O}_2])$.

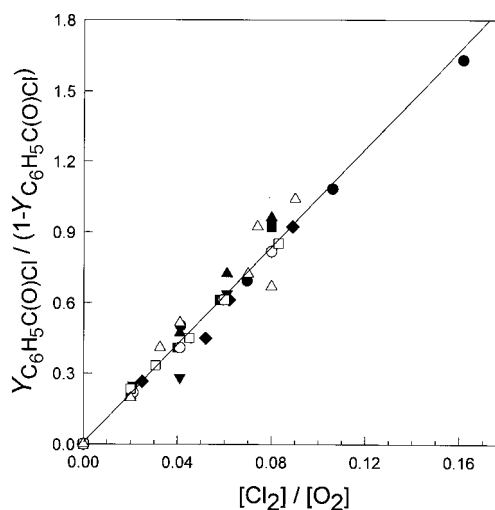
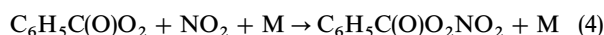


Fig. 3 Plot of $Y_{\text{C}_6\text{H}_5\text{C}(\text{O})\text{Cl}}/(1 - Y_{\text{C}_6\text{H}_5\text{C}(\text{O})\text{Cl}})$ *vs.* $[\text{Cl}_2]/[\text{O}_2]$ for experiments conducted at 1 (filled circles), 5 (filled squares), 10 (filled triangles), 50 (filled inverse triangles), 100 (filled diamonds), 200 (open circles), 500 (open squares), and 700 (open triangles) Torr total pressure and $296 \pm 2 \text{ K}$.

3.4 Relative reactivity of $C_6H_5C(O)O_2$ radicals towards NO and NO_2

The rate constant ratio k_3/k_4 was measured by subjecting mixtures of 6–9 mTorr of C_6H_5CHO , 70–80 mTorr of NO_x , 70–90 mTorr of Cl_2 , and 10–11 Torr of O_2 , in 700 Torr of N_2 diluent, to successive 15–20 s periods of UV irradiation:



The formation of benzoyl peroxybenzoyl nitrate [$C_6H_5C(O)O_2NO_2$] *via* reaction (4) was readily discernible by virtue of its characteristic IR features at 989, 1229, and 1739 cm^{-1} (ref. 6). A calibrated IR spectrum of $C_6H_5C(O)O_2NO_2$ was obtained by irradiating $C_6H_5CHO/Cl_2/NO_2/O_2$ mixtures. The product features at 989, 1229, and 1739 cm^{-1} ascribed to $C_6H_5C(O)O_2NO_2$ increased linearly with the loss of C_6H_5CHO , from which we derive $\sigma(989 \text{ cm}^{-1}) = 2.75 \times 10^{-18} \text{ cm}^2 \text{ molecule}^{-1}$, with an estimated uncertainty of $\pm 20\%$. The IR spectrum of $C_6H_5C(O)O_2NO_2$ measured here is shown in Fig. 4(A) and is qualitatively consistent with previous spectra reported by Heuss and Glasson,³ Gay *et al.*¹⁶ and Niki *et al.*¹⁷ As seen from Fig. 4(A), the IR absorption cross sections measured in the present work are significantly greater than those reported by Heuss and Glasson³ (circles) and Gay *et al.*¹⁶ (triangle). The magnitude of the discrepancy varies inversely with the spectral width of the IR features, indicating that these features were not fully resolved in the previous work. The spectral resolution used in the present work (0.25 cm^{-1}) is sufficient to fully resolve the band envelopes of all the IR features. For comparison the IR spectrum of $CH_3C(O)O_2NO_2$ measured recently at Ford¹⁸ is given in Fig. 4(B). The IR features of $CH_3C(O)O_2NO_2$ are broader than those of $C_6H_5C(O)O_2NO_2$ and the absorption cross sections measured at Ford¹⁸ and by Gay *et al.*¹⁶ (triangle) and Stephens¹⁹ (diamonds) are in good agreement.

Assuming that $C_6H_5C(O)O_2$ radicals are lost solely *via* reactions (3) and (4) and that the concentrations of NO and NO_2 do not change substantially during an experiment, then a plot of the reciprocal of the peroxybenzoyl nitrate yield ($1/Y_{RO_2NO_2}$) vs. the ratio of the average concentrations of NO and NO_2 in the chamber ($[NO]_{av}/[NO_2]_{av}$) should be linear

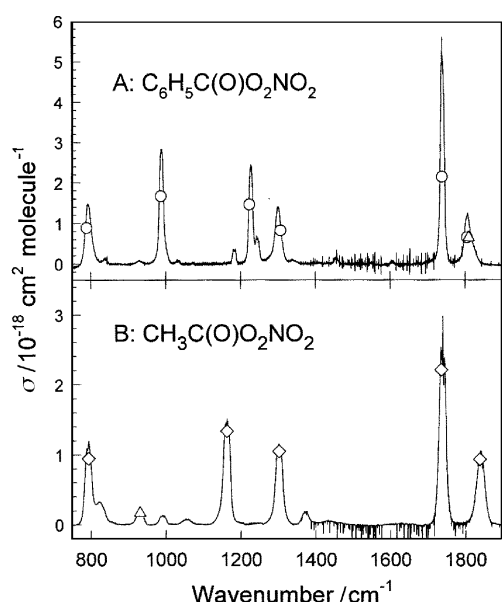


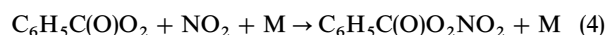
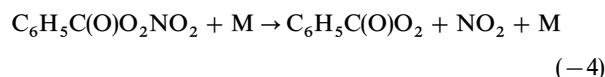
Fig. 4 IR spectra of $C_6H_5C(O)O_2NO_2$ (measured here) and $CH_3C(O)O_2NO_2$ (from ref. 18); circles are from ref. 3, triangles from ref. 16 and diamonds from ref. 19.

with a slope of k_3/k_4 and an intercept of unity. As seen from Fig. 5 linear behaviour was indeed observed. During the course of an experiment the NO and NO_2 concentrations changed by ≈ 1 –6%. In the calculation of $Y_{RO_2NO_2}$ values small corrections (7–9%) were applied to account for the formation of $C_6H_5C(O)Cl$ *via* reaction (10). Linear least squares analysis gives $k_3/k_4 = 1.44 \pm 0.15$. This result is somewhat lower than, but consistent within the experimental uncertainties with, the previous measurements of $k_3/k_4 = 1.52 \pm 0.12$ in 800 Torr of Ar at 303.6 K by Kenley and Hendry⁵ and $k_3/k_4 = 1.59 \pm 0.20$ in 1000 mbar of N_2 at 310–322 K by Kirchner *et al.*⁶

3.5 Thermal stability of $C_6H_5C(O)O_2NO_2$

The thermal stability of $C_6H_5C(O)O_2NO_2$ was studied in the smog chamber at Ford in 700 Torr total pressure of N_2/O_2 mixtures at 306.1, 301.2, and 293.0 K. To check for heterogeneous loss of $C_6H_5C(O)O_2NO_2$ in the chamber a mixture of $C_6H_5C(O)O_2NO_2$ in the presence of a large excess of NO_2 was left in the chamber in the dark for 10 min at 296 K. There was no loss (<1%) of $C_6H_5C(O)O_2NO_2$ suggesting the absence of complications caused by heterogeneous loss processes.

Addition of NO to reaction mixtures containing $C_6H_5C(O)O_2NO_2$ led to a decay of this species. In the presence of excess NO, the loss of $C_6H_5C(O)O_2NO_2$ was not dependent on the NO concentration and is not caused by a reaction between $C_6H_5C(O)O_2NO_2$ and NO. Instead, NO scavenges $C_6H_5C(O)O_2$ radicals formed in the thermal decomposition of $C_6H_5C(O)O_2NO_2$ thereby limiting its reformation *via* reaction (4):



As shown in the insert in Fig. 6 the decay of $C_6H_5C(O)O_2NO_2$ followed first order kinetics. Linear least-squares analysis of these data gives pseudo first order rate constants for the thermal decomposition of $C_6H_5C(O)O_2NO_2$. Regeneration of $C_6H_5C(O)O_2NO_2$ can occur *via* reaction (4). The observed pseudo first order rate constant for $C_6H_5C(O)O_2NO_2$ decay, k_{obs} , is related to k_{-4} , by the expression:

$$k_{-4} = k_{obs} \times \{1 + (k_4[NO_2]/k_3[NO])\}$$

The observed $C_6H_5C(O)O_2NO_2$ decay rate, k_{obs} , was corrected for regeneration *via* reaction (4) using $k_4/k_3 = 0.69$ (see

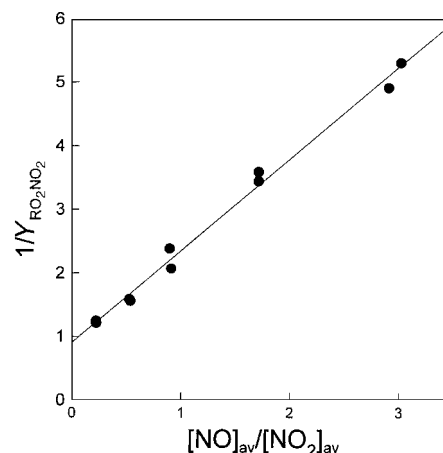


Fig. 5 Plot of $1/Y_{RO_2NO_2}$ vs. $[NO]_{av}/[NO_2]_{av}$ for experiments performed in 700 Torr total pressure at 296 K.

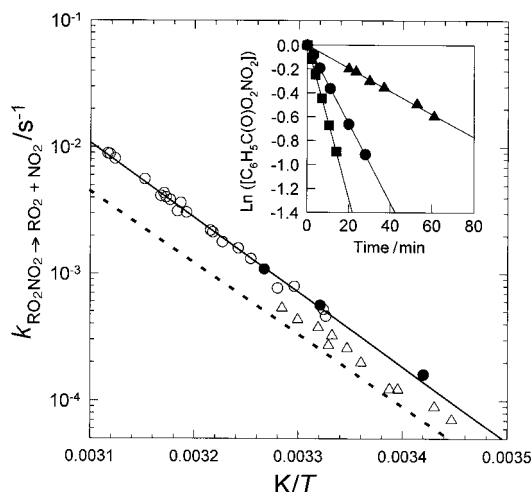


Fig. 6 Arrhenius plot for the thermal decomposition of $C_6H_5C(O)O_2NO_2$ measured in the present work in 700 Torr of air diluent (\bullet), by Kirchner *et al.*⁶ in 1000 mbar (750 Torr) of N_2 (\circ), and by Ohta and Mizoguchi²⁰ in 650 Torr of N_2/O_2 (Δ). The solid line is a linear least-squares fit to the combined data set from the present work and that of Kirchner *et al.*⁶ The dotted line is the Arrhenius expression derived by Kenley and Hendry.⁵ The insert shows the decay observed at the three temperatures studied here.

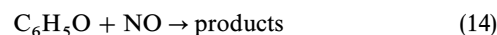
previous section). The concentrations of NO and NO_2 in the chamber were monitored using their characteristic IR absorptions. Corrections were in the range 2–10% and have been applied to the results from the present work indicated by the filled circles in the Arrhenius plot in Fig. 6. In 700 Torr of air at 306.1, 301.2, and 293.0 K values of k_{-4} were determined to be 1.09×10^{-3} , 5.62×10^{-4} , and $1.60 \times 10^{-4} s^{-1}$, respectively. The open symbols in Fig. 6 are the results reported by Kirchner *et al.*⁶ in 1000 mbar (750 Torr) of N_2 . As seen from Fig. 6 the results from the present work (filled circles) are in good agreement with those of Kirchner *et al.*⁶ (open circles). The solid line in Fig. 6 is a linear least-squares fit to the combined data set from Kirchner *et al.*⁶ and the present work, giving $k_{-4} = (2.1^{+5.0}_{-1.5}) \times 10^{16} \exp[-(13\,600 \pm 400) K/T] s^{-1}$. The triangles in Fig. 6 are the results reported by Ohta and Mizoguchi²⁰ which lie 30–40% below those obtained here and by Kirchner *et al.*⁶ When Ohta and Mizoguchi²⁰ conducted their work the rate constant ratio k_4/k_3 had yet to be measured and consequently no corrections were computed for the effect of regeneration of $C_6H_5C(O)O_2NO_2$ via reaction (4). Typical initial experimental conditions employed by Ohta and Mizoguchi²⁰ were 18 ppm $C_6H_5C(O)O_2NO_2$, 6 ppm NO_2 , and 83 ppm NO, and at the mid point of the $C_6H_5C(O)O_2NO_2$ decay the $[NO_2]/[NO]$ concentration ratio would have been approximately 0.5. Using $k_4/k_3 = 0.69$ it follows that the results of Ohta and Mizoguchi²⁰ need to be multiplied by a factor of approximately 1.35 to account for regeneration of $C_6H_5C(O)O_2NO_2$ via reaction (4). Application of such a correction factor would bring the results of Ohta and Mizoguchi²⁰ into agreement with those reported here and by Kirchner *et al.*⁶ The dotted line in Fig. 6 is the Arrhenius expression reported by Kenley and Hendry⁵ which, for unknown reasons, lies approximately a factor of 2 below our results.

3.6 FTIR product study of the reaction of peroxybenzoyl radicals with NO

To provide insight into the atmospheric chemistry of benzoyl-peroxy radicals product studies were performed using mixtures of 6–9 mTorr of benzaldehyde, 200–300 mTorr of Cl_2 , 16.6–45.9 mTorr of NO, in 700 Torr of air diluent at 296 K. Reaction mixtures were subjected to 3–7 successive irradiations

each having a duration of 2–5 s. After each irradiation the reaction mixtures were analysed using FTIR spectroscopy. In all experiments a substantial yield of CO_2 was observed by virtue of its characteristic IR features at 2200–2400 cm^{-1} . Fig. 7 shows a plot of the increase in CO_2 vs. the loss of benzaldehyde. The concentration of CO_2 increased linearly with the loss of benzaldehyde suggesting that CO_2 is formed as a primary product. Linear least-squares analysis gives a molar yield of CO_2 of $98 \pm 5\%$. Variation of the partial pressure of NO over the range 16.6–45.9 mTorr had no discernible impact on the yield of CO_2 .

The observation of CO_2 product in essentially 100% yield is consistent with the following reactions occurring in the system:



Reactions (14) and (15) proceed rapidly and are believed to give nitroso- and nitrophenols.^{17,21,22} Consistent with the previous study by Niki *et al.*¹⁷ of the Cl initiated oxidation of benzaldehyde in the presence of NO_x , residual IR product features at 748, 872, 1200, 1291, and 1342 cm^{-1} attributable to *o*- and *p*-nitrophenol were observed. Unfortunately, due to the low vapor pressure of these compounds, it was not possible to quantify the yield of these nitrophenols.

3.7 UV absorption spectrum and self reaction kinetics of the $C_6H_5C(O)O_2$ radical

Strong transient absorption signals were observed in the wavelength range 245–260 nm, upon flashing $Cl_2/C_6H_5CHO/O_2/N_2$ mixtures, and were assigned to the peroxybenzoyl radical. Fig. 8 shows a typical trace recorded on two different time scales using a monitoring wavelength of 250 nm. Experiments were not performed below 245 nm because of the intense absorption of the benzaldehyde precursor (see Fig. 9). For the experimental conditions used to record the traces in Fig. 8 ($[C_6H_5CHO] = 9 \times 10^{14}$, $[O_2] = 5 \times 10^{18}$ molecule cm^{-3}) the conversion of Cl atoms into $C_6H_5C(O)O_2$ radicals is complete in less than 25 μs . However, because of

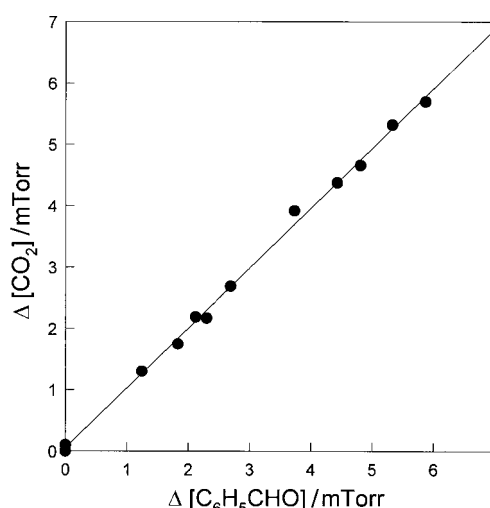


Fig. 7 Yields of CO_2 vs. loss of benzaldehyde observed following the UV irradiation of $C_6H_5CHO/Cl_2/NO/O_2/N_2$ mixtures.

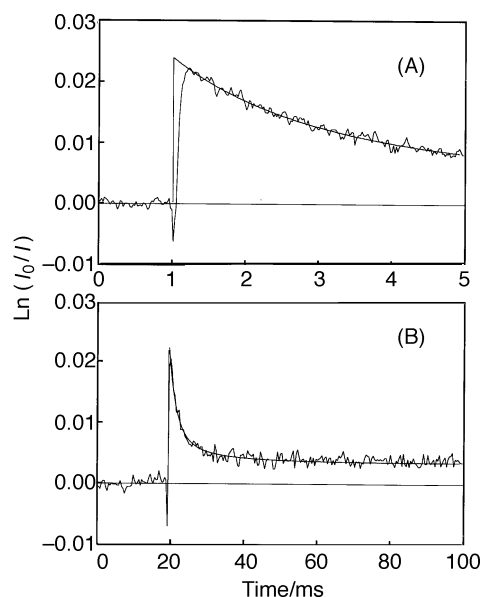


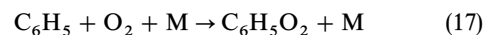
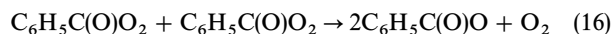
Fig. 8 Decay traces corresponding to the $C_6H_5C(O)O_2$ self reaction recorded at a monitoring wavelength of 250 nm, $T = 335$ K, 760 Torr air, $[Cl_2] = 2.0 \times 10^{16}$ molecule cm^{-3} , $[C_6H_5C(O)O_2]_0 = 2.2 \times 10^{13}$ molecule cm^{-3} using a 5 ms (A) or 100 ms (B) time scale. Smooth curves are best fit simulations.

the postflash dead time of the detection system the observed absorption shown in Fig. 8 does not reach a maximum until approximately 250 μs . To obtain an accurate UV spectrum for the $C_6H_5C(O)O_2$ radical it is necessary to extrapolate the transient signal back to zero time.

To make an accurate extrapolation, decay traces were simulated using the reaction mechanism given in Table 1, which is composed mainly of self and cross reactions of radicals. The rate of the peroxybenzoyl radical self reaction [reaction (16)] largely determines the initial shape of decay traces used for extrapolation to zero time and, consequently, both the UV spectrum and the k_{16} had to be determined simultaneously.

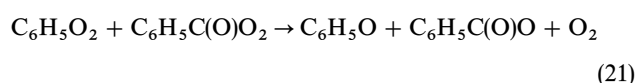
By analogy with the acetylperoxy radical self reaction it is assumed that the peroxybenzoyl radical self reaction yields benzyloxy radicals, $C_6H_5C(O)O$, which decompose liberating CO_2 and a phenyl radical, which can react with O_2 , Cl_2 or C_6H_5CHO . This is supported by the high yield of CO_2

(> 70%) observed in FTIR experiments in the absence of NO:



The reaction of C_6H_5 with O_2 proceeds at 298 K with a rate constant of 1.8×10^{-11} cm^3 molecule $^{-1}$ s $^{-1}$ (ref. 20). For the experimental conditions of $[O_2]/[Cl_2] > 100$ reaction (18) will not compete with reaction (17). The rate constant k_{19} has not been measured but it is likely to be of a similar magnitude to that of the corresponding reaction with HCHO (2.9×10^{-14} cm^3 molecule $^{-1}$ s $^{-1}$)²³ and will not be significant. For the initial radical concentrations used ($1-3 \times 10^{13}$ molecule cm^{-3}) all reactions of C_6H_5 with other radicals can be neglected.

The phenylperoxy radical self reaction and its cross reaction with $C_6H_5C(O)O_2$ were included in the mechanism:



The rate constants k_{20} and k_{21} were set at values typical for the self reaction of a secondary peroxy radical and its reaction with $CH_3(O)O_2$.²⁴ Reactions involving C_6H_5O radicals were taken from the literature.^{21,22}

The initial radical concentration was determined by replacing benzaldehyde by methane ($\approx 2 \times 10^{18}$ molecule cm^{-3}), recording the absorption by methylperoxy radicals, and using $\sigma_{CH_3O_2, 240\text{ nm}} = 4.55 \times 10^{-18}$ cm^2 molecule $^{-1}$ (ref. 25). Benzaldehyde absorbs significantly at the measurement wavelengths (see Fig. 9) and its absorption was accounted for using the cross sections given in Table 2. To obtain values for $\sigma(C_6H_5C(O)O_2)$ the initial part (0–4 ms) of the decay trace was modelled with $\sigma(C_6H_5C(O)O_2)$ and k_{16} varied to provide the best fit. As seen from Fig. 8, use of the data in Tables 1 and 2 gives an acceptable simulation of the decay trace and provides confidence in the extrapolation method. Values of $\sigma(C_6H_5C(O)O_2)$ obtained are given in Table 2 and plotted in Fig. 9.

In the long-wavelength part of the spectrum ($\lambda > 260$ nm), where $\sigma(C_6H_5C(O)O_2)$ decreases, an initial slight increase of

Table 1 Reaction mechanism

Reaction	Rate constant at 298 K (cm^3 molecule $^{-1}$ s $^{-1}$)	Ref.
$Cl_2 + hv \rightarrow Cl + Cl$		
$Cl + C_6H_5CHO \rightarrow HCl + C_6H_5CO$	9.6×10^{-11}	10
$C_6H_5CO + O_2 + M \rightarrow C_6H_5C(O)O_2 + M$	5.7×10^{-12}	15
$C_6H_5C(O)O_2 + C_6H_5C(O)O_2 \rightarrow 2C_6H_5C(O)O + O_2$	1.35×10^{-11}	This work
$C_6H_5C(O)O \rightarrow C_6H_5 + CO_2$	(assumed instantaneous)	
$C_6H_5 + O_2 + M \rightarrow C_6H_5O_2 + M$	(assumed instantaneous)	
$C_6H_5O_2 + C_6H_5O_2 \rightarrow C_6H_5O + C_6H_5O + O_2$	5.0×10^{-12}	assumed, see text
$C_6H_5O_2 + C_6H_5C(O)O_2 \rightarrow C_6H_5O + C_6H_5C(O)O + O_2$	1.0×10^{-11}	assumed, see text
$C_6H_5O + Cl_2 \rightarrow C_6H_5OCl + Cl$	1.0×10^{-14}	21
$C_6H_5O + C_6H_5O \rightarrow$ products	1.2×10^{-11}	21
$C_6H_5O + C_6H_5O_2 \rightarrow$ products	5.0×10^{-12}	assumed, see text
$C_6H_5O + C_6H_5C(O)O_2 \rightarrow$ products	2.0×10^{-11}	assumed, see text
$C_6H_5C(O)O_2 + NO \rightarrow C_6H_5C(O)O + NO_2$	1.60×10^{-11}	This work
$C_6H_5C(O)O_2 + NO_2 \rightarrow C_6H_5C(O)O_2NO_2$	1.11×10^{-11}	This work
$C_6H_5O_2 + NO \rightarrow C_6H_5O + NO_2$	7.0×10^{-12}	assumed, see text
$C_6H_5O_2 + NO_2 \rightarrow$ products	1.0×10^{-11}	assumed, see text
$C_6H_5O + NO \rightarrow C_6H_5ONO$	1.65×10^{-12}	21
$C_6H_5O + NO_2 \rightarrow$ products	2.1×10^{-12}	22

Table 2 UV absorption cross sections

λ/nm	$\sigma/10^{-18} \text{ cm}^2 \text{ molecule}^{-1}$				
	$\text{C}_6\text{H}_5\text{C}(\text{O})\text{O}_2^a$	$\text{C}_6\text{H}_5\text{O}_2^b$	$\text{C}_6\text{H}_5\text{COCl}^a$	$\text{C}_6\text{H}_5\text{CHO}^c$	$\text{C}_6\text{H}_5\text{O}^d$
245	20 ± 1	1.5	7.5	7.05	9.5
250	19.5 ± 1	2.0	1.9	2.75	8.6
255	19.5 ± 1	2.0	1.6	3.05	4.7
260	16.5 ± 1	2.5	2.1	3.65	2.0
265	11.5 ± 2	7.0	2.5		
270	9 ± 3	9.0	3.0	4.65	
280	7 ± 3	7.5	3.6	4.10	11.7
290	6 ± 4	7.0	1.2	2.10	9.2
300	4 ± 3	7.0	0.8	1.65	

^a This work. ^b Estimated from simulations of decay traces. ^c This work. ^d From ref. 21.

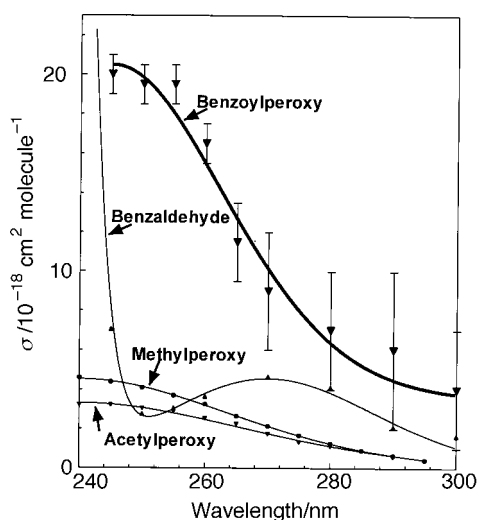


Fig. 9 UV absorption spectrum of the $\text{C}_6\text{H}_5\text{C}(\text{O})\text{O}_2$ radical. Spectra of benzaldehyde, $\text{CH}_3\text{C}(\text{O})\text{O}_2$ radicals, and CH_3O_2 radicals are shown for comparison.

the absorbance appeared before the decay. This indicates the formation of a product which absorbs more strongly than the peroxybenzoyl radical in this wavelength range. We tentatively assign this absorption to the $\text{C}_6\text{H}_5\text{O}_2$ radical. Values of $\sigma(\text{C}_6\text{H}_5\text{O}_2)$ needed to fit the absorption transients are given in Table 2. The error bars given for $\sigma(\text{C}_6\text{H}_5\text{C}(\text{O})\text{O}_2)$ over the region 270–300 nm reflect the additional uncertainties associated with the extrapolation.

The UV spectrum of the $\text{C}_6\text{H}_5\text{C}(\text{O})\text{O}_2$ radical measured here is compared with the spectra of $\text{CH}_3\text{C}(\text{O})\text{O}_2$ and CH_3O_2 radicals in Fig. 9. The spectra of $\text{CH}_3\text{C}(\text{O})\text{O}_2$ and CH_3O_2 over the wavelength range 240–300 nm are typical of organic peroxy radicals which have a broad featureless absorption band with a maximum at 240–250 nm of $(4\text{--}5) \times 10^{-18} \text{ cm}^2 \text{ molecule}^{-1}$. As seen from Fig. 9, the absorption spectrum of the $\text{C}_6\text{H}_5\text{C}(\text{O})\text{O}_2$ radical also appears to exhibit a maximum around 240–250 nm; however the spectrum is much more intense than that of a typical peroxy radical. The combined acyl and aromatic nature of this radical and the possibility of delocalization of the radical center is almost certainly responsible for this high absorption cross section. *Ab initio* calculations of the electron density of the $\text{C}_6\text{H}_5\text{C}(\text{O})\text{O}_2$ would be interesting but are beyond the scope of the present work.

Despite the assumptions and approximations inherent in the reaction mechanism (Table 1), the rate constant k_{16} for the $\text{C}_6\text{H}_5\text{C}(\text{O})\text{O}_2$ radical self reaction could be determined with fairly good confidence. The value of k_{16} is derived mainly from fitting the first part of the decay, whereas other reactions, which result from products of the self reaction, determine the shape of the trace at longer times. We estimate that the uncertainty in k_{16} is $\pm 20\%$.

Values of k_{16} measured at 298–460 K are listed in Table 3 and the corresponding Arrhenius plot is shown in Fig. 10. The resulting rate expression is:

$$k_{16} = (3.1 \pm 1.4) \times 10^{-13} \times \exp[(1110 \pm 160) \text{ K}/T] \text{ cm}^3 \text{ molecule}^{-1} \text{ s}^{-1}$$

giving

$$k_{16} = (1.3 \pm 0.6) \times 10^{-11} \text{ cm}^3 \text{ molecule}^{-1} \text{ s}^{-1} \text{ at } 298 \text{ K}$$

This value is similar to those reported for the acetylperoxy radical self reaction ($1.4\text{--}1.6 \times 10^{-11} \text{ cm}^3 \text{ molecule}^{-1} \text{ s}^{-1}$)^{24,26} and for the propionylperoxy radical $\text{C}_2\text{H}_5\text{C}(\text{O})\text{O}_2$ ($1.2 \times 10^{-11} \text{ cm}^3 \text{ molecule}^{-1} \text{ s}^{-1}$)²⁷ indicating that acylperoxy radical self reactions are all fast, with similar rate constants. In addition, similar rate constants have been found recently for the self reactions of the acylperoxy radicals $(\text{CH}_3)_2\text{CHC}(\text{O})\text{O}_2$ and $(\text{CH}_3)_3\text{CC}(\text{O})\text{O}_2$.²⁸ However, self reactions of perfluorinated acylperoxy radicals seem to have slightly lower rate constants, $9.1 \times 10^{-12} \text{ cm}^3 \text{ molecule}^{-1} \text{ s}^{-1}$ for $\text{CF}_3\text{C}(\text{O})\text{O}_2$ ²⁹ and $6.5 \times 10^{-12} \text{ cm}^3 \text{ molecule}^{-1} \text{ s}^{-1}$ for $\text{FC}(\text{O})\text{O}_2$.^{30,31}

Table 3 Experimental values of $k[\text{C}_6\text{H}_5\text{C}(\text{O})\text{O}_2 + \text{C}_6\text{H}_5\text{C}(\text{O})\text{O}_2]$

T/K	$k_{16}/10^{-11} \text{ cm}^3 \text{ molecule}^{-1} \text{ s}^{-1}$	No. of determinations
298	1.35 ± 0.3	8
325	0.9 ± 0.2	6
335	0.8 ± 0.2	3
350	0.8 ± 0.2	8
460	0.35 ± 0.2	2

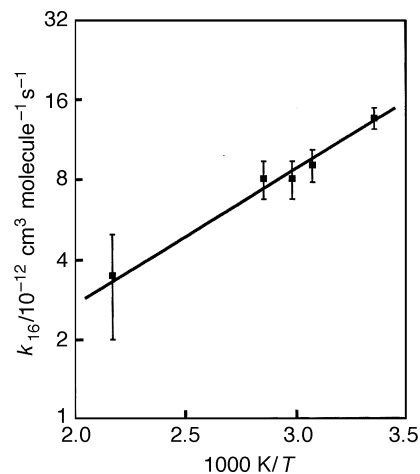


Fig. 10 Arrhenius plot for the $\text{C}_6\text{H}_5\text{C}(\text{O})\text{O}_2$ self reaction.

3.8 Kinetic study of the $C_6H_5C(O)O_2 + NO$ reaction

The reaction of the peroxybenzoyl radical with NO was investigated using the flash photolysis of $C_6H_5CHO/O_2/Cl_2/NO/N_2$ mixtures. Measurements were performed in 760 Torr of air at (338 ± 4) K where the handling of benzaldehyde was most convenient (see Section 2.2). As expected, the peroxybenzoyl decay rate increased significantly in the presence of NO, as shown in Fig. 11.

All experiments were performed under pseudo first order conditions, using an excess of NO. The concentration of NO was varied over the range $(7-23) \times 10^{13}$ molecule cm^{-3} . The pseudo first order rate constant was optimised for each concentration of NO by simulation of decay traces, performed using the reaction mechanism described above together with the reactions of $C_6H_5C(O)O_2$, $C_6H_5O_2$, and C_6H_5O radicals with NO and NO_2 (Table 1). The results are listed in Table 4 and plotted in Fig. 12 giving $k_3 = (1.6 \pm 0.4) + 10^{-11}$ cm^3 molecule $^{-1}$ s $^{-1}$ in 760 Torr of air at 338 K. The quoted uncertainty represents both the statistical uncertainty in the regression analysis of the data in Fig. 12 together with an estimate of the likely uncertainties associated with fitting the decay traces using the mechanism in Table 1. Our result for k_3 is indistinguishable from the corresponding rate constant for reaction of acetylperoxy radicals with NO of $(1.79 \pm 0.05) \times 10^{-11}$ cm^3 molecule $^{-1}$ s $^{-1}$ at 338 K (ref. 32). In its reaction with NO the $C_6H_5C(O)O_2$ radical behaves like a typical acetylperoxy radical. As noted above, for experimental convenience, measurements of k_3 were performed at (338 ± 4) K. Based upon the kinetic data base for reactions of peroxy radicals with NO,¹⁴ the kinetics of the reaction of $C_6H_5C(O)O_2$ with NO are not expected to change substantially (<10%) between 338 K and ambient temperature. It

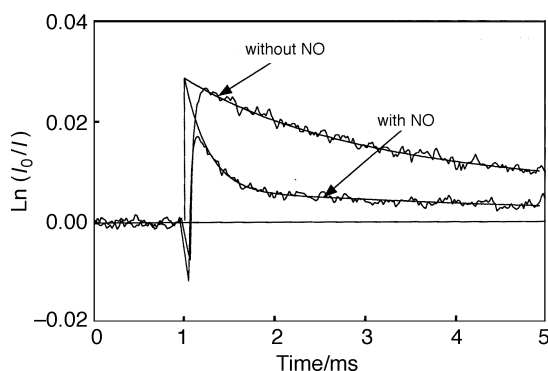


Fig. 11 Typical experimental traces obtained in the absence and in the presence of NO, in 760 Torr air, at a monitoring wavelength of 250 nm and $T = 338$ K: $[C_6H_5CHO] = 1.1 \times 10^{15}$ molecule cm^{-3} , $[Cl_2] = 2.0 \times 10^{16}$ molecule cm^{-3} ; $[O_2] = 4.9 \times 10^{18}$ molecule cm^{-3} ; $[NO] = 1.52 \times 10^{14}$ molecule cm^{-3} . Solid lines are the best fit simulations.

Table 4 Results for the $C_6H_5C(O)O_2 + NO$ reaction

$[NO]/10^{13}$ molecule cm^{-3}	$k_3 \times [NO]/s^{-1}$ ^a
6.89	1310 ± 210
7.14	1140 ± 220
11.1	1890 ± 330
11.4	1820 ± 350
15.2	2690 ± 300
15.8	2690 ± 600
15.8	2220 ± 470
19.5	2930 ± 590
23	3680 ± 580
23	3450 ± 690

^a Errors are estimated from uncertainties on simulation parameters.

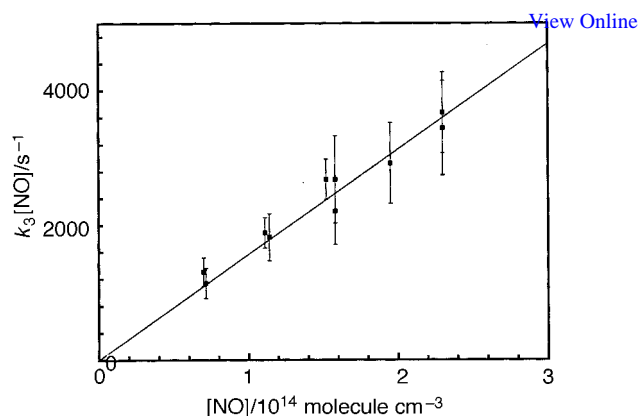


Fig. 12 Decay rate of $C_6H_5C(O)O_2$ vs. $[NO]$: $T = (338 \pm 4)$ K, 760 Torr air.

seems reasonable to assume that the value of $k_3 = (1.6 \pm 0.4) \times 10^{-11}$ cm^3 molecule $^{-1}$ s $^{-1}$ will be applicable to ambient temperature.

4 Discussion

A large body of data concerning the atmospheric chemistry of benzaldehyde is presented here. The atmospheric degradation of benzaldehyde is initiated by reaction with OH radicals during the day and NO_3 radicals at night. Both reactions proceed predominantly *via* abstraction of the aldehydic H atom to give $C_6H_5C(O)$ radicals. In one atmosphere of air the sole fate of $C_6H_5C(O)$ radicals is addition of O_2 to give $C_6H_5C(O)O_2$ radicals which occurs with a pseudo first order rate constant of 3×10^7 s $^{-1}$ (ref. 15). In polluted air masses, the fate of $C_6H_5C(O)O_2$ radicals is reaction with NO_x (NO and NO_2). Typical NO_x concentrations in moderately polluted urban air are 1–10 ppbV. Using $k_3 = 1.1 \times 10^{-11}$ and $k_4 = 1.6 \times 10^{-11}$ cm^3 molecule $^{-1}$ s $^{-1}$ measured here, it follows that in typical urban air masses the lifetime of $C_6H_5C(O)O_2$ radicals with respect to reaction with NO_x is approximately 0.2–4.0 s. As shown here, the reaction of $C_6H_5C(O)O_2$ radicals with NO leads to the formation of CO_2 and, by inference, C_6H_5 radicals, in 100% yield. Reaction of $C_6H_5C(O)O_2$ radicals with NO_2 produces a peroxybenzoyl radical which decomposes with a rate constant of $k_{-4} = 2.1 \times 10^{16} \exp(-13600 \text{ K}/T)$ s $^{-1}$ (lifetime with respect to thermal decomposition of ≈ 1 h at 298 K, ≈ 2 days at 273 K, and ≈ 16 days at 263 K). Phenyl radicals produced following reaction of $C_6H_5C(O)O_2$ radicals with NO will be converted by reactions (12) and (13) into phenoxy radicals (C_6H_5O). Phenoxy radicals react rapidly with NO (refs. 21, 22), NO_2 (ref. 22), and O_3 (ref. 33). Using $k(NO) = 1.65 \times 10^{-12}$, $k(NO_2) = 2.1 \times 10^{-12}$, and $k(O_3) = 2.86 \times 10^{-13}$ cm^3 molecule $^{-1}$ s $^{-1}$, and NO_x and O_3 concentrations in moderately polluted urban air of 1–10 ppbV and 0–100 ppb, respectively, it follows that these reactions are competitive loss mechanisms for phenoxy radicals. The reactions of phenoxy radicals with NO and NO_2 leads to the formation of nitroso- and nitrophenols.¹⁷ These reactions remove both NO_x and a radical species and are probably responsible for the well known negative incremental reactivity of benzaldehyde (*i.e.* addition of benzaldehyde to a hydrocarbon- NO_x -air mixture decreases oxidant formation.^{1,34,35} The mechanism of the reaction of phenoxy radicals with ozone is unknown; further work is needed in this area.

Acknowledgements

FC, VF and RL wish to thank the Commission of the European Union for financial support within the "Environment and Climate" Programme. We thank Marchoe Dill for help with the experiments conducted at Ford.

References

- 1 J. H. Seinfeld and S. N. Pandis, *Atmospheric Chemistry and Physics*, John Wiley & Sons, Inc., New York, 1998.
- 2 J. R. Odum, T. P. W. Jungkamp, R. J. Griffin, R. C. Flagan and J. H. Seinfeld, *Science*, 1997, **276**, 96.
- 3 J. M. Heuss and W. A. Glasson, *Environ. Sci. Technol.*, 1968, **12**, 1109.
- 4 R. Atkinson, *J. Phys. Chem. Ref. Data*, 1984, **13**, 315.
- 5 R. A. Kenley and D. G. Hendry, *J. Am. Chem. Soc.*, 1982, **104**, 220.
- 6 F. Kirchner, F. Zabel and K. H. Becker, *Chem. Phys. Lett.*, 1992, **191**, 169.
- 7 T. J. Wallington, C. A. Gierczak, J. C. Ball and S. M. Japar, *Int. J. Chem. Kinet.*, 1989, **21**, 1077.
- 8 P. D. Lightfoot, R. Lesclaux and B. Veyret, *J. Phys. Chem.*, 1990, **94**, 700.
- 9 W. B. DeMore, M. J. Molina, S. P. Sander, D. M. Golden, R. F. Hampson, M. J. Kurylo, C. J. Howard, C. E. Kolb and A. R. Ravishankara, *Chemical Kinetics and Photochemical Data for Use in Stratospheric Modelling*, NASA-JPL Publication 97-4, Jet Propulsion Laboratory, Pasadena, 1997.
- 10 B. Nozière, R. Lesclaux, M. D. Hurley, M. A. Dearth and T. J. Wallington, *J. Phys. Chem.*, 1994, **98**, 2864.
- 11 T. J. Wallington and M. D. Hurley, *Chem. Phys. Lett.*, 1992, **189**, 437.
- 12 T. E. Møgelberg, A. Feilberg, A. M. B. Giessing, J. Sehested, T. J. Wallington and O. J. Nielsen, *J. Phys. Chem.*, 1995, **99**, 17386.
- 13 E. W. Kaiser and T. J. Wallington, *J. Phys. Chem.*, 1995, **99**, 8669.
- 14 W. G. Mallard, F. Westley, J. T. Herron, R. F. Hampson and D. H. Frizzell, *NIST Chemical Kinetics Database*, Version 6.0, NIST, Gaithersburg, MD, 1994.
- 15 C. E. Dade, T. M. Lenhart and K. D. Bayes, *J. Photochem.*, 1982, **20**, 1.
- 16 B. W. Gay, R. C. Noonan, J. J. Bufalini and P. L. Hanst, *Environ. Sci. Technol.*, 1976, **10**, 82.
- 17 H. Niki, P. D. Maker, C. M. Savage and L. P. Breitenbach, Fourier transform infrared (FTIR) studies of gaseous and particulate nitrogenous compounds, in *Nitrogenous Air Pollutants*, ed. D. Grosjean, Ann Arbor Science Publishers, Ann Arbor, MI, 1979.
- 18 J. Sehested, L. K. Christensen, T. E. Møgelberg, O. J. Nielsen, T. J. Wallington and A. Guschin, *J. Phys. Chem. A*, 1998, **102**, 1779.
- 19 E. R. Stephens, *Anal. Chem.*, 1964, **36**, 928.
- 20 T. Ohta and I. Mizoguchi, *Environ. Sci. Technol.*, 1981, **15**, 1229.
- 21 F. Berho, F. Caralp, M. T. Rayez, R. Lesclaux and E. Ratajczak, *J. Phys. Chem. A*, 1998, **102**, 1.
- 22 J. Platz, O. J. Nielsen, T. J. Wallington, J. C. Ball, M. D. Hurley, A. M. Straccia, W. F. Schneider and J. Sehested, *J. Phys. Chem. A*, 1998, **102**, 7964.
- 23 T. Yu and M. C. Lin, *J. Am. Chem. Soc.*, 1993, **115**, 4371.
- 24 R. Lesclaux, in *Peroxy Radicals*, ed. Z. E. Alfassi, John Wiley & Sons, Ltd., New York, 1997.
- 25 F. G. Simon, W. Schneider and G. K. Moorgat, *Int. J. Chem. Kinet.*, 1990, **22**, 791.
- 26 M. M. Maricq, J. J. Szente, G. A. Khitrov and J. S. Francisco, *J. Phys. Chem.*, 1996, **100**, 4514.
- 27 I. Bridier, PhD Thesis, Bordeaux, 1991.
- 28 A. Tomas, E. Villenave and R. Lesclaux, Proceedings of the second workshop of EUROTRAC 2 subproject: "Chemical Mechanism Development" (GPP27), Karlsruhe, Germany, 1998, to be published.
- 29 M. M. Maricq and J. J. Szente, *J. Phys. Chem.*, 1996, **100**, 4507.
- 30 M. M. Maricq, J. J. Szente, G. A. Khitrov and J. S. Francisco, *J. Phys. Chem.*, 1993, **98**, 9522.
- 31 T. J. Wallington, T. Ellermann, O. J. Nielsen and J. Sehested, *J. Phys. Chem.*, 1994, **98**, 2346.
- 32 J. Sehested, L. K. Christensen, T. E. Møgelberg, O. J. Nielsen, T. J. Wallington, A. G. Guschin, J. J. Orlando and G. S. Tyndall, *J. Phys. Chem. A*, 1998, **102**, 1779.
- 33 Z. Tao and Z. Li, *Int. J. Chem. Kinet.*, 1999, **29**, 65.
- 34 R. L. Kuntz, S. L. Kopczynski and J. J. Bufalini, *Environ. Sci. Technol.*, 1973, **7**, 1119.
- 35 W. P. L. Carter and R. Atkinson, *Environ. Sci. Technol.*, 1987, **21**, 670.

Paper 9/03088C